

Regular Texture Analysis as Statistical Model Selection

Junwei Han, Stephen J. McKenna, and Ruixuan Wang

School of Computing, University of Dundee, Dundee DD1 4HN, UK

{[jeffhan](mailto:jeffhan@computing.dundee.ac.uk), [stephen](mailto:stephen@computing.dundee.ac.uk), [ruixuanwang](mailto:ruixuanwang@computing.dundee.ac.uk)}@computing.dundee.ac.uk

<http://www.computing.dundee.ac.uk>

Abstract. An approach to the analysis of images of regular texture is proposed in which lattice hypotheses are used to define statistical models. These models are then compared in terms of their ability to explain the image. A method based on this approach is described in which lattice hypotheses are generated using analysis of peaks in the image autocorrelation function, statistical models are based on Gaussian or Gaussian mixture clusters, and model comparison is performed using the marginal likelihood as approximated by the Bayes Information Criterion (BIC). Experiments on public domain regular texture images and a commercial textile image archive demonstrate substantially improved accuracy compared to two competing methods. The method is also used for classification of texture images as regular or irregular. An application to thumbnail image extraction is discussed.

1 Introduction

Regular texture can be modelled as consisting of repeated texture elements, or *texels*. The texels tessellate (or tile) the image (or more generally a surface). Here we consider so-called wallpaper patterns. Wallpaper patterns can be classified into 17 groups depending on their symmetry [1]. Translationally symmetric regular textures can always be generated by a pair of shortest vectors (two linearly independent directions), \mathbf{t}_1 and \mathbf{t}_2 , that define the size, shape and orientation (but not the position) of the texel and the lattice which the texel generates. The lattice topology is always then quadrilateral. Geometric deformations, varying illumination, varying physical characteristics of the textured surface, and sensor noise all result in images of textured patterns exhibiting approximately regular, as opposed to exactly regular, texture. This paper considers the problem of automatically inferring texels and lattice structures from images of planar, approximately regular textures viewed under orthographic projection. While this might at first seem restrictive, this problem is, as will become apparent, far from solved. There exists no fully automatic and robust algorithm to the best of the authors' knowledge. Furthermore, solutions will find application, for example in analysis, retrieval and restoration of images of printed textiles, wallpaper and tile designs.

1.1 Related Work

Extraction of periodicity plays an important role in understanding texture and serves as a key component in texture recognition [2], synthesis [3] and segmentation [4]. Previous work proposed for texel and lattice extraction can be grouped broadly into two categories: the local feature-based approach [5,6,7,8,9,10,11] and the global structure-based approach [1,12,13,14,15,16]. All texture analysis is necessarily both local and global. The categorisation is in terms of the computational approach: whether it starts by identifying local features and proceeds to analyse global structure, or starts with a global analysis and proceeds by refining estimates of local structure.

The local feature-based approach starts by identifying a number of texel candidates. Matching based on visual similarity between these potential texels and their neighbours is then performed. Successful matching leads to the connection of texels into a lattice structure. The approach iterates until no more new texels are found. Methods vary in the way they initialise texel candidates and in the parametric models used to cope with geometric and photometric variation. Lin et al. [6] asked users to provide an initial texel. Interest points and edges have been used to generate texel candidates automatically [7,8,9]. However, Hays et al. [5] pointed out that interest points often fail to find texel locations and instead initialized by combining interest points and normalized cross correlation patches. Affine models have been adopted to deal with local variation among texels [7,10,11]. Global projective transformation models have also been used, taking advantage of the spatial arrangement of texels [8,9]. Hays et al. [5] formulated lattice detection as a texel correspondence problem and performed texel matching based on visual similarity and geometric consistency. Lin et al. [6] proposed a Markov random field model with a lattice structure to model global topological relationships among texels and an image observation model able to handle local variations.

The global structure-based approach [1,12,13,14,15,16] tries to extract texels using methods that emphasise the idea of periodic patterns as global processes. Starovoitov et al. [16] used features derived from cooccurrence matrices to extract texels. Charalampidis et al. [15] used a Fourier transform and made use of peaks corresponding to fundamental frequencies to identify texels. The autocorrelation (AC) function is generally more robust than the Fourier transform for the task of texel extraction especially in cases in which a regular texture image contains only a few texel repetitions [1,12]. Peaks in the AC function of a regular texture image can identify the shape and arrangement of texels. Chetverikov [13] developed a regularity measure by means of finding the maximum over all directions on the AC function. Leu [14] used the several highest peaks in the AC function computed on the gradient field of the image to capture translation vectors. A promising approach was presented by Lin et al. [12] in which salient peaks were identified using Gaussian filters to iteratively smooth the AC function. The generalized Hough transform was then applied to find translation vectors, \mathbf{t}_1 and \mathbf{t}_2 . Liu et al. [1] highlighted the fact that spurious peaks often result in incorrect lattice vectors. Therefore, they proposed a “region of dominance” operator to

select a list of dominant peaks. The translation vectors were estimated based on these dominant peaks. However, the important problem of how to determine the number of dominant peaks was not addressed. Whilst it is usually relatively easy for a human to select an appropriate subset of peaks, automating this process is difficult. Fig. 1 shows three different texels obtained similarly to Lin et al. [12] from the same image by using different numbers of peaks. The peaks were obtained using the region of dominance method [1]. Whilst using only the first ten peaks can result in success, the method is rather sensitive to this choice.

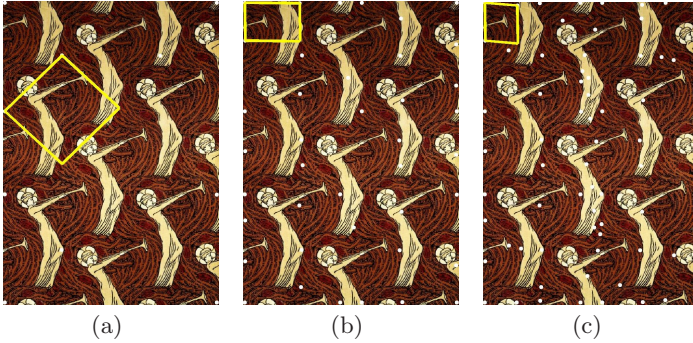


Fig. 1. Texels obtained using (a) ten, (b) forty, and (c) seventy dominant peaks in the autocorrelation function. The peak locations are marked with white dots.

Available local feature-based methods can be effective under significant texture surface deformation and are more suited to such situations. However, they require texels that can be identified based on local features (such as corners) and perform matching between individual texels. Therefore they often fail to detect larger, non-homogeneous texels. Fig. 2 shows examples of such failures.

Global structure-based methods are suitable for textures that do not exhibit large geometric deformation and often successfully identify larger texels with more complicated appearances. However, existing methods have free parameters



Fig. 2. Two examples of a local feature-based method [5] extracting incorrect lattices

for which a fixed value that works on a wide range of images can often not be found. Methods based on finding peaks in an AC function often yield many unreliable peaks and the number which are reliable can vary dramatically between images. This serious drawback currently makes these methods difficult to apply to large image collections.

1.2 Contributions

We propose a novel model comparison framework to test texel hypotheses and find the optimal one. Hypotheses can be constructed using existing methods according to different subsets of AC peaks by varying the number of peaks used. A statistical model is defined for each lattice hypothesis. The most probable hypothesis given the image observation will be selected. The design of the statistical model takes account of photometric and (to a lesser extent) geometric variations between texels. Hence, our method is robust and completely automatic.

The contributions of this paper can be summarized as follows. (i) A Bayesian model comparison framework is proposed to extract texels from regular texture images based on statistical models defined to handle variations between texels. (ii) Lattice comparison is also used to classify texture images as regular or irregular. (iii) Empirical comparison of the proposed method with two existing methods is performed on a challenging regular texture image database. (iv) The method is applied to generate smart thumbnails for an image browsing and retrieval system.

The rest of this paper is organized as follows. Section 2 presents the Bayesian model comparison framework. Section 3 describes details of lattice model comparison. Section 4 describes the method used in our experiments for generating lattice hypotheses. Experimental results are given in Section 5. An application in which the proposed method is used to generate smart thumbnails for regular texture images is reported in Section 6. Finally, conclusions are drawn in Section 7.

2 Bayesian Model Comparison Framework

Our approach is to formulate texel hypotheses as statistical models and then compare these models given the image data. It is not sufficient for a model to be able to fit the data well. The best texel hypothesis under this criterion would be the image itself whereas our purpose is to extract the smallest texture element. Therefore, overfitting must be guarded against by penalising model complexity. Texel hypothesis comparison can be regarded as a typical model comparison problem for unsupervised statistical modelling of data. Such a problem can be formulated as Bayesian model comparison which naturally penalises complexity (Occam's razor).

Let $I = \{x_1, x_2, \dots, x_N\}$ be an image with N pixels. Here, $x_n, 1 \leq n \leq N$ is the intensity of the n^{th} pixel. Let $H \equiv (\mathbf{t}_1, \mathbf{t}_2)$ denote a texel hypothesis for I , H_k the k^{th} in a set of hypotheses, and M_k a statistical model defined based on H_k with parameters θ_k . Texel extraction can be formulated as choosing the

most probable texel hypothesis given the image. According to Bayes' theorem, the posterior probability is proportional to the likelihood of the hypothesis times a prior:

$$p(H_k|I) = \frac{p(I|H_k)p(H_k)}{p(I)} \propto p(I|H_k)p(H_k) \quad (1)$$

In the absence of prior knowledge favouring any of the texel hypotheses, the (improper) prior is taken to be uniform. For each H_k , we define a unique M_k deterministically so $p(M_k|H_k)$ is a delta function. Hence,

$$p(H_k|I) \propto p(I|M_k) = \int p(I|\theta_k, M_k)p(\theta_k|M_k)d\theta_k \quad (2)$$

Texel hypotheses can be compared by comparing the marginal likelihoods, $p(I|M_k)$, for their models. Here $p(I|\theta_k, M_k)$ is the probability density function of the image data given the model M_k and its parameters θ_k , and $p(\theta_k|M_k)$ is the prior probability density function of parameters θ_k given the model M_k .

The integral in Equation (2) can only be computed analytically in certain cases such as exponential likelihoods with conjugate priors. Otherwise, approximations can be obtained using sampling methods, for example. While it would be interesting to explore these alternatives in future work, this paper uses the Bayes Information Criterion (BIC) as a readily computable approximation. BIC approximates the marginal likelihood integral via Laplace's method and the reader is referred to the papers by Schwarz [17] and Raftery [18] for full details of its derivation. Given a maximum likelihood parameter estimate, $\hat{\theta}$, we have

$$\log p(I|M) \approx \log p(I|\hat{\theta}, M) + \log p(\hat{\theta}) + \frac{d}{2} \log 2\pi - \frac{d}{2} \log N - \frac{1}{2} \log |\mathbf{i}| + O(N^{-1/2}) \quad (3)$$

where d is the number of parameters and \mathbf{i} is the expected Fisher information matrix for one observation. The subscript k has been dropped here for clarity. The term $\log p(I|\hat{\theta}, M)$ is of order $O(N)$, $(d/2) \log N$ is of order $O(\log N)$, and the remaining terms are of order $O(1)$ or less. The log marginal likelihood can be approximated by removing all terms of order $O(1)$ or less. The BIC for the model is then

$$BIC(M) = -\log p(I|\hat{\theta}, M) + (d/2) \log N \approx -\log p(I|M_k) \quad (4)$$

The first term can be interpreted as an error of fit to the data while the second term penalises model complexity.

The proposed approach to regular texture analysis involves (i) generation of multiple texel hypotheses, and (ii) comparison of hypotheses based on statistical models. The hypothesis with the model that has the largest marginal likelihood is selected. Using the BIC approximation, hypothesis $H_{\hat{k}}$ is selected where,

$$\hat{k} = \arg \max_k \{p(H_k|I)\} = \arg \min_k \{BIC(M_k)\} \quad (5)$$

This method can also be used to classify textures as regular or irregular. If a ‘good’ lattice can be detected in an image then it should be classified as regular. The proposed lattice comparison framework can be adopted for this purpose by comparing the most probable lattice found with a reference hypothesis in which the entire image is a single ‘texel’. If the reference hypothesis has a higher BIC value then the image is classified as regular. Otherwise, it is classified as irregular, i.e.

$$\begin{aligned} BIC(M_R) \leq BIC(M_{\hat{k}}) & \quad \text{Irregular texture} \\ BIC(M_R) > BIC(M_{\hat{k}}) & \quad \text{Regular texture} \end{aligned} \tag{6}$$

where M_R refers to the model corresponding to the reference lattice and $M_{\hat{k}}$ is the best lattice hypothesis selected by Equation (5).

3 Lattice Models

The lattice model should be able to account for both regularity from periodic arrangement and statistical photometric and geometric variability. Let us first suppose a regular texture image I with N pixels x_1, x_2, \dots, x_N , and a hypothesis H with Q pixels per texel. Based on H , each pixel of the image is assigned to one of Q positions on the texel according to the lattice structure. Thus, the N pixels are partitioned into Q disjoint sets, or clusters. If we choose to assume that the N pixels are independent given the model, we have,

$$p(I|M) = \prod_{n=1}^N p(x_n|M) = \prod_{q=1}^Q \prod_{n:f(n,H)=q} p(x_n|M) \tag{7}$$

where $f(n, H) \in \{1, \dots, Q\}$ maps n to its corresponding index in the texel. Fig. 3 illustrates this assignment of pixels to clusters.

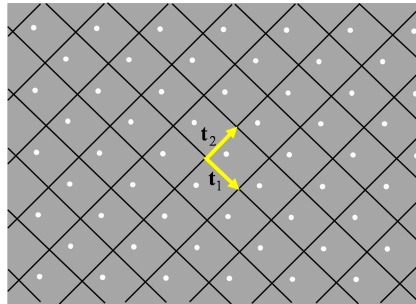


Fig. 3. An example of cluster allocation according to a texel hypothesis, $H \equiv (\mathbf{t}_1, \mathbf{t}_2)$. The value of $f(n, H)$ is the same for each of the highlighted pixels. There are Q pixels in each parallelogram.

Modelling each of the Q clusters as Gaussian with fixed variance gives:

$$BIC(M) = (Q/2) \log N - \sum_{q=1}^Q \sum_{n: f(n,H)=q} \log p(x_n | \hat{\mu}_q, \sigma^2) \quad (8)$$

$$= (Q/2) \log N + C_1 + \frac{1}{2\sigma^2} \sum_{q=1}^Q \sum_{n: f(n,H)=q} (x_n - \hat{\mu}_q)^2 \quad (9)$$

where C_1 is a constant that depends on σ^2 , and $\hat{\mu}_q$ is a maximum likelihood estimate of the mean of the q^{th} cluster.

Alternatively, a more heavy-tailed distribution can be used for each cluster. This might better model outliers due to physical imperfections in the texture surface and variations due to small geometric deformations. For example, a cluster can be modelled as a mixture of two Gaussians with the same mean but different variances, (σ_1^2, σ_2^2) , and a mixing weight, π_1 that places greater weight on the low variance Gaussian. In that case,

$$BIC(M) = - \sum_{q=1}^Q \sum_{n: f(n,H)=q} \log p(x_n | \hat{\mu}_q, \sigma_1^2, \sigma_2^2, \pi_1) + (Q/2) \log N \quad (10)$$

$$= (Q/2) \log N + C_2 \quad (11)$$

$$- \sum_{q=1}^Q \sum_{n: f(n,H)=q} \log \left(\frac{\pi_1}{\sigma_1} \exp \frac{-(x_n - \hat{\mu}_q)^2}{2\sigma_1^2} + \frac{1 - \pi_1}{\sigma_2} \exp \frac{-(x_n - \hat{\mu}_q)^2}{2\sigma_2^2} \right)$$

where C_2 is a constant.

4 Lattice Hypothesis Generation

In principle, there is an unlimited number of lattice hypotheses. However, probability density will be highly concentrated at multiple peaks in the hypothesis space. The posterior distribution can therefore be well represented by only considering a, typically small, number of hypotheses at these peaks. In the maximum a posteriori setting adopted here, the approach taken is to identify multiple hypotheses in a data-driven manner and then compare these hypotheses using BIC. The approach is general in that any algorithms that generate a variety of reasonable hypotheses can be used.

In the experiments reported here, aspects of the methods of Lin et al. [12] and Liu et al. [1] were combined to generate hypotheses. Peaks in AC functions are associated with texture periodicity but automatically deciding which peaks can characterize the arrangement of texels is problematic and has not been properly addressed in the literature [1,12,13,14]. In particular, changing the number of peaks considered can result in different lattice hypotheses. Since the total number of peaks is limited, we can only obtain a limited number of hypotheses.

Given a grey-scale image $I(x, y)$, $1 \leq x \leq L$, $1 \leq y \leq W$ where L and W are image height and width, its AC function can be computed as follows:

$$AC(x, y) = \frac{\sum_{i=1}^L \sum_{j=1}^W I(i, j)I(i + x, j + y)}{\sum_{i=1}^L \sum_{j=1}^W I^2(i, j)} \quad (12)$$

Applying the fast Fourier transform (FFT) to calculate the AC function is a more efficient alternative.

$$AC(x, y) = F^{-1}[F[I(x, y)] * F[I(x, y)]] \quad (13)$$

where F and F^{-1} denote FFT and inverse FFT, respectively.

Lin et al. [12] used iterative smoothing with Gaussian filters to obtain salient peaks. However, Liu et al. [1] advised to take into account the spatial relationships among peaks and used a “region of dominance” operator. The basic idea behind this operator is that peaks that dominate large regions of the AC function are more perceptually important. In this paper, we combine these two algorithms. First, we apply Gaussian filters to iteratively smooth the AC function. Then, salient peaks obtained from the first stage are ranked according to their dominance. The most highly ranked peaks are selected as input for lattice hypothesis construction using a Hough transform [12]. The number of peaks in the rank-ordered list to use was varied in order to generate multiple hypotheses. Typically a few tens of the generated hypotheses will be distinct.

5 Experiments

A dataset of 103 regular texture images was used for evaluation, comprising 68 images of printed textiles from a commercial archive and 35 images taken from three public domain databases (the Wikipedia Wallpaper Groups page, a Corel database, and the CMU near regular texture database). These images ranged in size from 352×302 pixels to 2648×1372 pixels. The number of texel repeats per image ranged from 5 to a few hundreds. This data set includes images that are challenging because of (i) appearance variations among texels, (ii) small geometric deformations, (iii) texels that are not distinctive from the background and are large non-homogeneous regions, (iv) occluding labels, and (v) stains, wear and tear in some of the textile images.

Systematic evaluations of lattice extraction are lacking in the literature. We compared the proposed method with two previously published algorithms. Two volunteers (one male and one female) qualitatively scored and rank ordered the algorithms. In cases of disagreement, they were forced to reach agreement through discussion. (Disagreement happened in very few cases).

When the proposed method used Gaussians to model clusters, the only free parameter was the variance, σ^2 . A suitable value for σ^2 was estimated from a set of 20 images as follows. Many texel hypotheses were automatically generated using different numbers of AC peaks and a user then selected from them the best translation vectors, $\mathbf{t}_1, \mathbf{t}_2$. Pixels were allocated to clusters according to

the resulting lattice and a maximum likelihood estimation of σ^2 was computed. The result was $\sigma^2 = 264$. Since this semi-automatic method might not be using precise texel estimates, it might overestimate the variance compared to that which would be obtained using optimal lattices. Therefore, further values for σ^2 (100, 144 and 196) were also used for evaluation in order to test the sensitivity of the method. In any particular experiment, σ^2 was fixed for all 103 test images. The method was also evaluated using a Gaussian mixture to model each cluster, with free parameters set to $\sigma_1^2 = 60$, $\sigma_2^2 = 800$, and $\pi_1 = 0.9$.

The observers were shown lattices overlaid on images and were asked to label each lattice as obviously correct (OC), obviously incorrect (OI), or neutral. They were to assign OC if the lattice was exactly the same or very close to what they expected, OI if the result was far from their expectations, and *neutral* otherwise. The presentation of results to the observers was randomised so as to hide from them which algorithms produced which results. The proposed method was compared with two related algorithms [12,1]. Liu et al. [1] did not specify how to determine the number of peaks in the autocorrelation function. Results are reported here using three different values for the number of peaks, namely 10, 40, and 70. Table 1 summarises the results. It seems clear that the method proposed in this paper has superior accuracy to the two other methods. The value of σ^2 had little effect on the results. Fig. 4 shows some examples of lattices obtained. The two images displayed in the first row have clear intensity variations between texels. The two examples in the second row have labels in the image and appearance varies among texels. Examples shown in rows 3 to 5 contain large non-homogenous texels. The left example in the last row is a *neutral* result. This example has a significant geometric deformation among texels. The right example in the last row is an *OI* result since it did not find the smallest texel.

Table 1. Comparison of proposed algorithm with related algorithms. Accuracy is defined as the number of OC results divided by the total number of test images.

Algorithm variant	# OC results	# OI results	# Neutral results	Accuracy
Gaussian ($\sigma^2 = 100$)	83	9	11	0.81
Gaussian ($\sigma^2 = 144$)	83	14	6	0.81
Gaussian ($\sigma^2 = 196$)	82	14	7	0.80
Gaussian ($\sigma^2 = 264$)	79	18	6	0.77
Gaussian mixture	81	17	5	0.79
Liu et al. [1] (10 peaks)	45	54	4	0.44
Liu et al. [1] (40 peaks)	50	47	6	0.49
Liu et al. [1] (70 peaks)	28	70	5	0.27
Lin et al. [12]	22	70	11	0.21

A further experiment was performed to compare the proposed method to the two other methods. For each image, lattice results from our algorithm using Gaussians, our algorithm using Gaussian mixtures, the algorithm of Liu et al. [1], and the algorithm of Lin et al. [12], respectively, were shown on the screen simultaneously. The two subjects rank ordered those four results. Algorithms

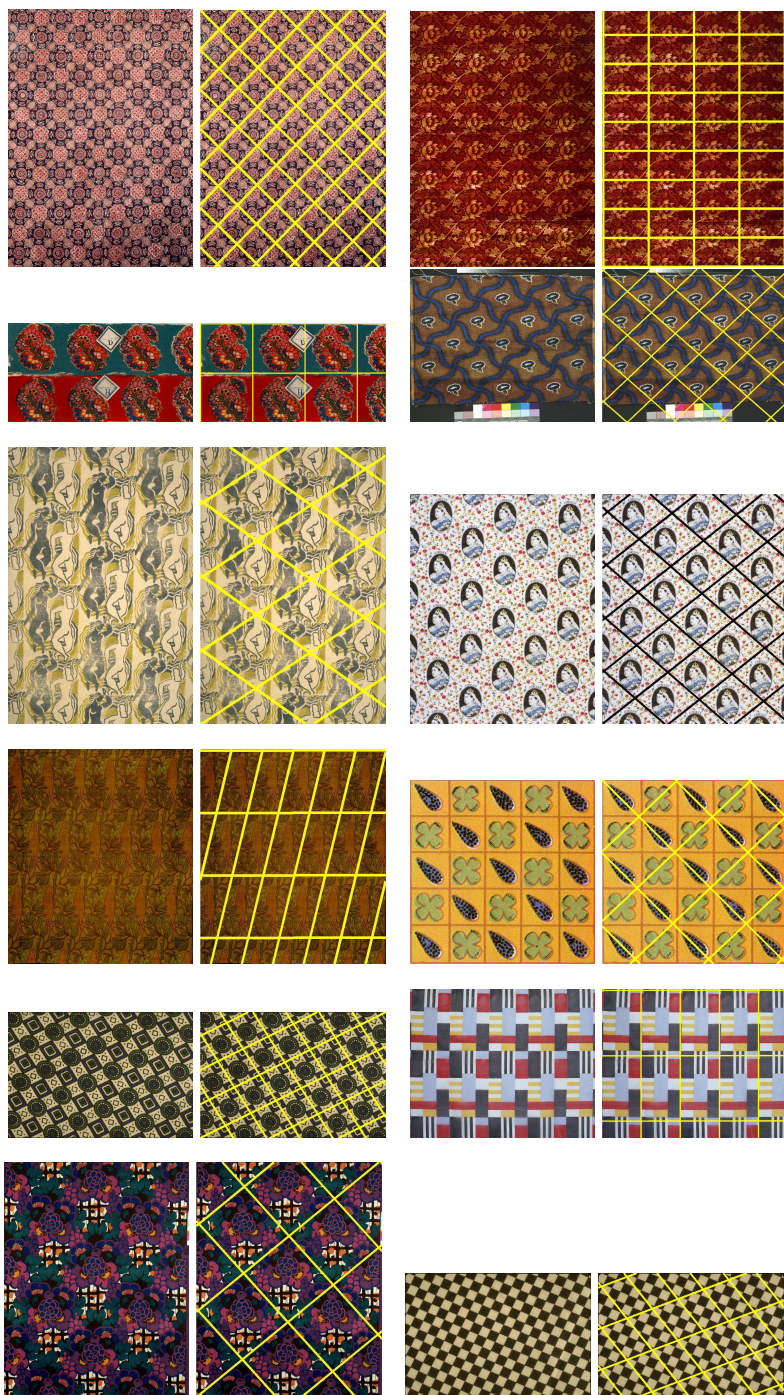


Fig. 4. Results from the proposed algorithm using Gaussian models

shared the same rank if they yielded equally good results. For example, if three of the algorithms gave good lattices of equal quality and the fourth algorithm gave a poor lattice then three algorithms shared rank 1 and the other algorithm was assigned rank 4. Table 2 summarizes the rankings. For the Gaussian model, we set $\sigma^2 = 264$ which yields the worst accuracy of the variance values tried. For the algorithm of Liu et al. [1], we set the number of dominant peaks to 40, which achieved the best performance of the values tried. Even with these parameter settings which disadvantage the proposed method, Table 2 shows that it is superior to the other algorithms.

Table 2. Comparisons by ranking results of different algorithms

Algorithm	# Rank 1	# Rank 2	# Rank 3	# Rank 4
Gaussian, $\sigma^2 = 264$	83	12	6	2
Gaussian mixture	86	11	5	1
Liu et al. [1] (# peaks = 40)	56	5	23	19
Lin et al. [12]	18	2	24	59

The method was also used to classify texture images as regular or irregular as described in Equation (6). A set of 62 images was selected randomly from a museum fine art database and from the same commercial textile archive as used earlier. Figure 5 shows some examples of these images. A classification experiment



Fig. 5. Examples of images to be classified as having *irregular* texture

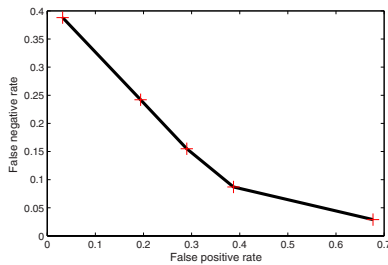


Fig. 6. Classification of texture as regular or irregular. The curve was plotted by varying the value of σ^2 and characterises the trade-off between the two types of error.

was performed using these images as negative examples and the 103 regular texture images as positive examples. Figure 6 shows the ROC curve obtained by varying the value of σ^2 in the Gaussian model ($\sigma^2 \in \{49, 64, 81, 100, 144\}$). The equal error rate was approximately 0.22.

The computational speed depends on the number of lattice hypotheses (and many different subsets of peaks lead to the same lattice hypothesis). A Matlab implementation typically takes a few minutes per image on a 2.4GHz, 3.5GB PC which is adequate for off-line processing.

6 Smart Thumbnail Generation for Regular Texture Images

Thumbnail images are widely used when showing lots of images on a display device of limited size. Most traditional approaches generate thumbnails by directly sub-sampling the original image which often reduces the recognisability of meaningful objects and patterns in the image. Suh et al. [19] developed a novel thumbnail generation method by taking into account human visual attention. A saliency map and a face detector were used to identify regions expected to attract visual attention. Although this method is effective for many images, it is not appropriate for images with regular texture that often comprise abstract patterns.

In an informal experiment, 9 human observers of varied age were asked to draw a rectangle on each of 14 regular texture images to delineate the region they would like to see as a thumbnail on a limited display. Most users tended to select regions a little larger than a single texel, or containing a few texels. This suggests that thumbnails might usefully be generated from regular texture images automatically by cropping based on texel extraction. Currently, we are exploring the use of such thumbnails for content-based image browsing and retrieval. Thumbnails are generated by cropping a rectangular sub-image that bounds a region a little larger than a texel, $(1.5\mathbf{t}_1, 1.5\mathbf{t}_2)$. Fig. 7 compares two thumbnails generated in this way with the standard method of directly reducing

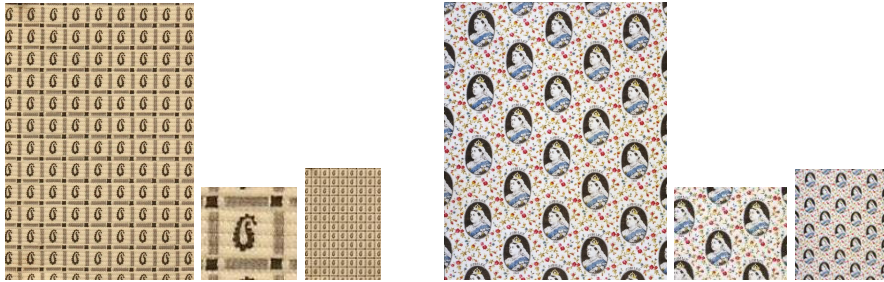


Fig. 7. Comparisons of two thumbnail generation methods. In each set, the first image is the original image, the second image is the thumbnail generated by our method, and the third image is the thumbnail generated by the standard method.

the resolution. Thumbnails extracted using knowledge of the texels can convey more detailed information about the pattern design.

7 Conclusions

A fully automatic lattice extraction method for regular texture images has been proposed using a framework of statistical model selection. Texel hypotheses were generated based on finding peaks in the AC function of the image. BIC was adopted to compare various hypotheses and to select a ‘best’ lattice. The experiments and comparisons with previous work have demonstrated the promise of the approach. Various extensions to this work would be interesting to investigate in future work. Alternative methods for generating hypotheses could be explored in the context of this approach. Further work is needed to explore the relative merits of non-Gaussian models. This should enable better performance on images of damaged textiles, for example. BIC can give poor approximations to the marginal likelihood and it would be worth exploring alternative approximations based on sampling methods, for example. Finally, it should be possible in principle to extend the approach to analysis of near-regular textures on deformed 3D surfaces by allowing relative deformation between texels. This could be formulated as a Markov random field over texels, for example. Indeed, Markov random field models have recently been applied to regular texture tracking [6].

Acknowledgments. The authors thank J. Hays for providing his source code, and Chengjin Du and Wei Jia for helping to evaluate the algorithm. This research was supported by the UK Technology Strategy Board grant “FABRIC: Fashion and Apparel Browsing for Inspirational Content” in collaboration with Liberty Fabrics Ltd., System Simulation Ltd. and Calico Jack Ltd. The Technology Strategy Board is a business-led executive non-departmental public body, established by the government. Its mission is to promote and support research into, and development and exploitation of, technology and innovation for the benefit of UK business, in order to increase economic growth and improve the quality of life. It is sponsored by the Department for Innovation, Universities and Skills (DIUS). Please visit www.innovateuk.org for further information.

References

1. Liu, Y., Collins, R.T., Tsin, Y.: A computational model for periodic pattern perception based on frieze and wallpaper groups. *IEEE Transactions on Pattern Analysis and Machine Intelligence* 26, 354–371 (2004)
2. Leung, T., Malik, J.: Recognizing surfaces using three-dimensional textons. In: *IEEE International Conference on Computer Vision*, Corfu, Greece, pp. 1010–1017 (1999)
3. Liu, Y., Tsing, Y., Lin, W.: The promise and perils of near-regular texture. *International Journal of Computer Vision* 62, 145–159 (2005)
4. Malik, J., Belongie, S., Shi, J., Leung, T.: Textons, contours and regions: cue integration in image segmentation. In: *IEEE International Conference of Computer Vision*, Corfu, Greece, pp. 918–925 (1999)

5. Hays, J., Leordeanu, M., Efros, A., Liu, Y.: Discovering texture regularity as a higher-order correspondence problem. In: European Conference on Computer Vision, Graz, Austria, pp. 533–535 (2006)
6. Lin, W., Liu, Y.: A lattice-based MRF model for dynamic near-regular texture tracking. *IEEE Transactions on Pattern Analysis and Machine Intelligence* 29, 777–792 (2007)
7. Leung, T., Malik, J.: Detecting, localizing and grouping repeated scene elements from an image. In: European Conference on Computer Vision, Cambridge, UK, pp. 546–555 (1996)
8. Tuytelaars, T., Turina, A., Gool, L.: Noncombinational detection of regular repetitions under perspective skew. *IEEE Transactions on Pattern Analysis and Machine Intelligence* 25, 418–432 (2003)
9. Schaffalitzky, F., Zisserman, A.: Geometric grouping of repeated elements within images. In: *Shape, Contour and Grouping in Computer Vision*. Lecture Notes In Computer Science, pp. 165–181. Springer, Heidelberg (1999)
10. Forsyth, D.A.: Shape from texture without boundaries. In: European Conference in Computer Vision, Copenhagen, Denmark, pp. 225–239 (2002)
11. Lobay, A., Forsyth, D.A.: Recovering shape and irradiance maps from rich dense texton fields. In: *Computer Vision and Pattern Recognition*, Washington, USA, pp. 400–406 (2004)
12. Lin, H., Wang, L., Yang, S.: Extracting periodicity of a regular texture based on autocorrelation functions. *Pattern Recognition Letters* 18, 433–443 (1997)
13. Chetverikov, D.: Pattern regularity as a visual key. *Image and Vision Computing* 18, 975–985 (2000)
14. Leu, J.: On indexing the periodicity of image textures. *Image and Vision Computing* 19, 987–1000 (2001)
15. Charalampidis, D.: Texture synthesis: Textons revisited. *IEEE Transactions on Image Processing* 15, 777–787 (2006)
16. Starovoitov, V., Jeong, S.Y., Park, R.: Texture periodicity detection: features, properties, and comparisons. *IEEE Transactions on Systems, Man, and Cybernetics-A* 28, 839–849 (1998)
17. Schwarz, G.: Estimating the dimensions of a model. *Annals and Statistics* 6, 461–464 (1978)
18. Raftery, A.E.: Bayesian model selection in social research. *Sociological Methodology* 25, 111–163 (1995)
19. Suh, B., Ling, H., Benderson, B.B., Jacobs, D.W.: Automatic thumbnail cropping and its effectiveness. In: *ACM Symposium on User Interface Software and Technology*, pp. 95–104 (2003)